Neuron, Vol. 38, 213–224, April 24, 2003, Copyright ©2003 by Cell Press

Lack of Enhanced Spinal Regeneration in Nogo-Deficient Mice

Binhai Zheng,[1] Carole Ho,[1] Shuxin Li,[2] Hans Keirstead,[3] Oswald Steward,[3] and Marc Tessier-Lavigne[1,*]
[1]Department of Biological Sciences
Howard Hughes Medical Institute
Stanford University
Stanford, California 94305
[2]Department of Neurology
Yale University School of Medicine
New Haven, Connecticut 06520
[3]Reeve-Irvine Research Center
Gillespie Neuroscience Research Facility
College of Medicine
University of California, Irvine
Irvine, California 92697

Summary

The failure of regeneration of severed axons in the adult mammalian central nervous system is thought to be due partly to the presence of endogenous inhibitors of axon regeneration. The *nogo* gene encodes three proteins (Nogo-A, -B, and -C) that have been proposed to contribute to this inhibition. To determine whether deletion of *nogo* enhances regenerative ability, we generated two lines of mutant mice, one lacking Nogo-A and -B but not -C (Nogo-A/B mutant), and one deficient in all three isoforms (Nogo-A/B/C mutant). Although Nogo-A/B-deficient myelin has reduced inhibitory activity in a neurite outgrowth assay in vitro, tracing of corticospinal tract fibers after dorsal hemisection of the spinal cord did not reveal an obvious increase in regeneration or sprouting of these fibers in either mouse line, suggesting that elimination of Nogo alone is not sufficient to induce extensive axon regeneration.

Introduction

During development, neuronal axons, tipped by growth cones, extend from their cell bodies of origin to reach their synaptic targets. In the adult, traumatic injury can lead to the severing of axons and thus to loss of functional connections. The distal portion of the axon, disconnected from the neuronal cell body, undergoes degeneration ("Wallerian degeneration") over several weeks. The proximal portion, in contrast, rapidly initiates a regenerative response: the cut end of the axon reseals itself, re-forms a growth cone like those on embryonic axons, and attempts to re-extend (Ramon y Cajal, 1928). In the mammalian peripheral nervous system (PNS), this regeneration can often be successful. In the mammalian central nervous system (CNS, the brain and spinal cord), however, the attempted regeneration fails, and the cut axon tips assume a club-like morphology ("end bulbs") that are thought to reflect a failed attempt at elongation (Ramon y Cajal, 1928; Schwab and Bartholdi, 1996).

Axonal regeneration following spinal cord injury is believed to be prevented by multiple factors, including a reduced propensity of adult CNS axons for axonal growth (Fawcett, 1992; Goldberg et al., 2002), the absence of some positive factors in the environment of the injured adult CNS (Jakeman and Reier, 1991), and the presence of inhibitory factors that actively block axonal regrowth (Schwab and Bartholdi, 1996). The development of therapies for axonal regeneration will require overcoming these inhibitory influences. There is evidence for multiple extracellular inhibitors contributing to inhibition block. Factors associated with the lesion site and scar tissue, including proteoglycans (Fitch and Silver, 1997) and possibly members of the semaphorin family (Pasterkamp et al., 1999), are believed to contribute significantly (Bradbury et al., 2002). Factors associated with the myelin sheath of axons, made by oligodendrocytes, have also been proposed to be an important source of inhibition (Schwab and Caroni, 1988). The first characterized inhibitor from myelin was myelin-associated glycoprotein (MAG), a potent inhibitor of axon growth in vitro (McKerracher et al., 1994; Mukhopadhyay et al., 1994). In vivo, however, loss of MAG function fails to promote extensive regeneration (Bartsch et al., 1995; Li et al., 1996), prompting the search for additional myelin-associated inhibitors.

The second inhibitor from myelin to be characterized molecularly was Nogo-A (Spillmann et al., 1998; Chen et al., 2000; GrandPré et al., 2000; Prinjha et al., 2000). Much interest has focused on this protein and its possible involvement in inhibition of axonal regeneration because of evidence that in vivo delivery of antibodies against Nogo can help stimulate regeneration of axons and compensatory sprouting and enhance functional recovery in animal models of spinal cord injury (Schnell and Schwab, 1990; Bregman et al., 1995; Thallmair et al., 1998; Brosamle et al., 2000). Although provocative, these studies left a number of questions unanswered, especially regarding the cellular and molecular basis of the growth inhibition.

First, it is not obvious how Nogo-A could operate as an extracellular inhibitor in the uninjured nervous system. It has two transmembrane domains but no signal sequence, and it possesses an endoplasmic reticulum (ER) retention sequence (Chen et al., 2000; GrandPré et al., 2000; Prinjha et al., 2000). Indeed, most Nogo protein appears localized to an intracellular compartment in cells (perhaps the ER) (GrandPré et al., 2000). This localization seems at odds with a possible involvement in inhibition of regeneration. The protein could be accessible to axons if it is released from dying oligodendrocytes following injury, but this would only explain growth inhibition in circumscribed regions where those cells are dying. It could contribute to growth inhibition in undamaged areas only if some of the protein is present on the myelin surface, a possibility for which some evidence has been obtained (GrandPré et al., 2000; Huber et al., 2002).

*Correspondence: marctl@stanford.edu

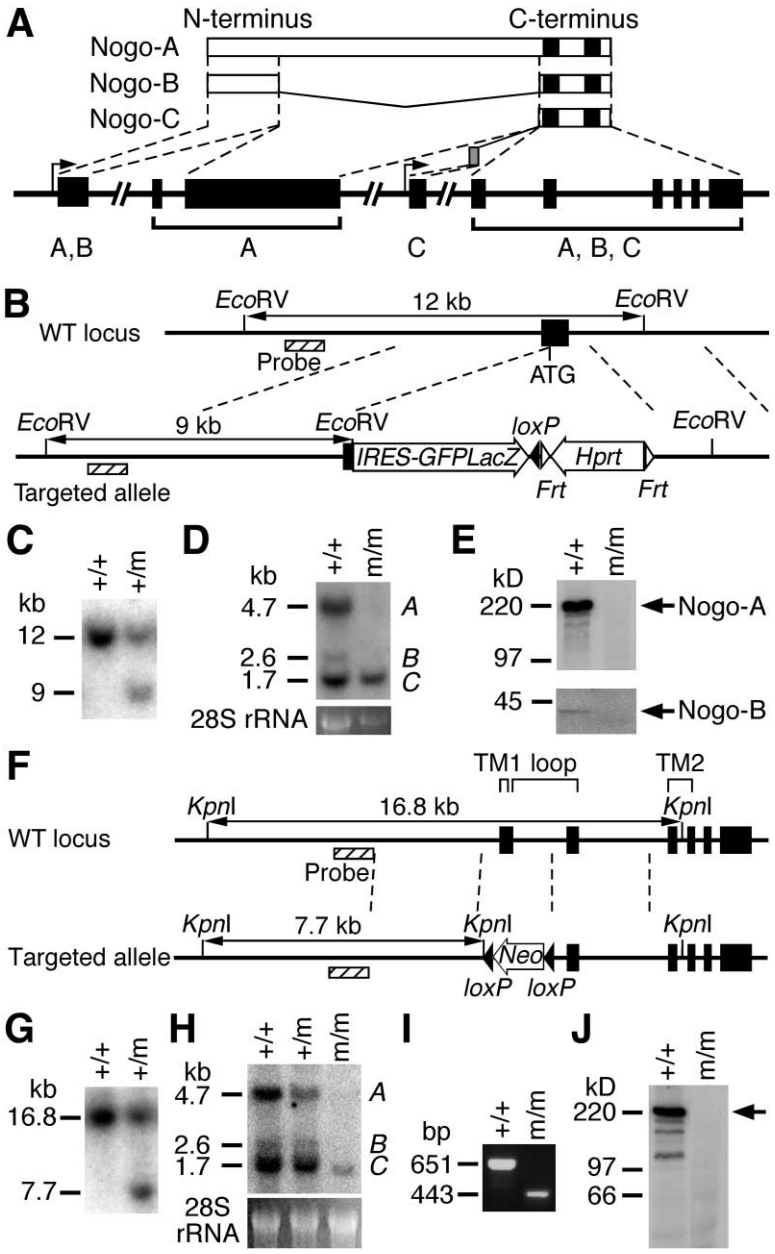

Figure 1. Generation of Nogo-A/B Mutant and Nogo-A/B/C Mutant Mice

(A) Structure of the murine *nogo* gene in relation to the three isoforms. Top: three Nogo isoforms. The two black bars in the C-terminal common region represent the two transmembrane domains that are separated by a 66 amino acid loop. Bottom: *nogo* genomic structure. The black bars indicate exons. Arrows indicate promoter regions. Nogo-A and -B share a promoter while Nogo-C has an alternative promoter.

(B–E) Targeting the N terminus of Nogo to generate the Nogo-A/B mutant.

(B) Targeting strategy for the Nogo-A/B mutant. WT, wild-type; *IRES,* internal ribosomal entry site; *GFP*, green fluorescent protein gene; *LacZ*, β-galatosidase gene; *Hprt*, hypoxanthine phosphoribosyltransferase gene under the control of the *PGK* (phosphoglycerate kinase) gene promoter; *TK*, *Herpes Simplex Virus thymidine kinase* gene. *loxP* and *frt* sites (recognized by Cre and Flp site-specific recombinases, respectively) are introduced into the targeted allele to facilitate further manipulation of the targeted locus.

(C) Southern analysis of ES cell DNA to identify the targeted clones. +, wild-type allele; m, mutant allele.

(D) Northern analysis of total brain RNA from wild-type and homozygous Nogo-A/B mutant mice using a probe corresponding to the coding portion of the C-terminal common region of *nogo* cDNA. *nogo-A, -B,* and *-C* transcripts run at about 4.7 kb, 2.6 kb, and 1.7 kb, respectively.

(E) Western blots on total adult brain extracts using anti-Nogo antibodies (top, anti-Nogo-A; bottom, anti-Nogo N terminus, to detect Nogo-B).

(F–J) Targeting the C terminus of Nogo to generate the Nogo-A/B/C mutant.

(F) Targeting strategy for the Nogo-A/B/C mutant. *Neo*, neomycin resistance gene under the control of the *PGK* promoter. TM, transmembrane domain.

(G) Southern analysis of ES cell DNA to identify the targeted clones.

(H) Northern analysis of total brain RNA from wild-type, heterozygous, and homozygous Nogo-A/B/C mutant mice (derived from the escaper) using the same probe as in (D). Note the presence of a lower level of a shortened Nogo-C transcript in the homozygous mutant (see text).

(I) RT-PCT analysis on *nogo-C* transcripts in wild-type and Nogo-A/B/C mutant mice using a primer set that specifically amplifies Nogo-C transcripts.

(J) Western blot analysis on total brain extract of wild-type and homozygous mutant adult mice using the anti-Nogo-A antibody. Arrow indicates the position of Nogo-A.

Second, there is controversy regarding the portion(s) of the Nogo molecule that mediates axonal inhibition. There are three major isoforms (A, B, and C) of Nogo arising by alternative splicing and promoter usage (Figure 1A; Chen et al., 2000; GrandPré et al., 2000; Prinjha et al., 2000). The largest, Nogo-A, has a long amino-terminal extension that possesses inhibitory activity (Chen et al., 2000; Prinjha et al., 2000; Fournier et al., 2001), but which has been proposed to be localized in the cytoplasm (GrandPré et al., 2000), making its function in inhibition in vivo unclear—unless it is somehow also present on the cell surface (Chen et al., 2000). Adding to the paradox, the in vivo experiments that suggested a role of Nogo in regeneration (Schnell and Schwab, 1990; Bregman et al., 1995; Thallmair et al., 1998; Brosamle et al., 2000) involved the IN-1 monoclonal antibody (Caroni and Schwab, 1988), which is apparently directed against an epitope in this extension (Chen et al., 2000). A second inhibitory domain has been localized to a 66 amino acid lumenal/extracellular loop in the portion of the Nogo protein that is common to all three isoforms (A, B, and C) (GrandPré et al., 2000), and

which is the target for a receptor protein (Nogo-66R or NgR) found on axons (Fournier et al., 2001). This portion of Nogo is on the appropriate (i.e., lumenal or extracellular) side of the membrane to be involved in inhibition. It is unclear, however, how much of the inhibitory actions of myelin is contributed by this domain, since antibodies against the long amino-terminal domain of Nogo-A were found to block completely the inhibitory action of myelin fractions containing Nogo-A in a sensory neurite outgrowth assay (Chen et al., 2000). A possible role for this domain in inhibition in vivo is consistent with the finding that a peptide that interferes with the interaction of Nogo-A and Nogo-66R can promote axonal regeneration in the injured adult spinal cord when administered in vivo (GrandPré et al., 2002). However, this result does not conclusively implicate the 66 amino acid loop, since NgR has recently been found also to be a receptor for both MAG (Liu et al., 2002; Domeniconi et al., 2002) and another recently identified inhibitory protein in myelin, oligodendrocyte-myelin glycoprotein (OMgp) (Wang et al., 2002). Thus, the peptide may have produced some of its effects by interfering with those ligands—or with other as yet unidentified inhibitory ligands for the receptor—rather than Nogo itself.

To clarify the role of Nogo in inhibition of axon regeneration in vivo and the domains important for inhibition, we generated mice that either lack Nogo-A and -B (but not -C) or that carry a C-terminal mutation that disrupts all three isoforms, and we assessed the regenerative response of CNS axons to spinal cord injuries. Our results reveal no evidence for enhanced regeneration in these animals.

Results

Generation of Nogo-A/B Mutant Mice

Figure 1A shows the structure of the *nogo* gene, assessed by characterizing genomic clones isolated from a mouse 129S5 genomic library and through analysis of genomic sequence from databases. The *nogo* gene spans over 50 kB and contains an A/B-specific exon (exon 1), two A-specific exons, one C-specific exon, and six A/B/C common exons.

To address the role of the long amino-terminal extension of Nogo, we generated a Nogo N-terminal mutation in which the A and B isoforms are specifically mutated, and only the C isoform remains. This mutation deletes an amino-terminal genomic fragment including the entire coding region of exon 1 downstream of the ATG start codon (Figure 1B) and is expected to completely abolish Nogo-A and Nogo-B expression. The targeted allele was obtained in AB2.2 ES cells (derived from strain 129S7) (Figure 1C), which was then used to generate chimeric mice. Heterozygous mutants were obtained by breeding chimeric mice to C57BL/6 females, and the mutation was backcrossed to C57BL/6 one more time before being homozygosed. In intercrosses between (C57BL/6 × 129S7) N2 heterozygotes, wild-type, heterozygous, and homozygous progeny appeared in Mendelian ratios (10 +/+, 22 +/m, and 10 m/m out of 5 litters). Homozygous mutants were viable, fertile, and morphologically indistinguishable from their wild-type littermates. Northern blot analysis of brain tissue from adult homozygous mice confirmed the absence of transcripts corresponding to Nogo-A and -B and the maintained presence of the -C isoform (Figure 1D). Western blot analysis using anti-Nogo antibodies demonstrated the absence of Nogo-A and Nogo-B proteins in the mutant brain (Figure 1E). Similarly, immunostaining of transverse sections from adult spinal cord using the anti-Nogo-A antibody confirmed the absence of Nogo-A in the mutant (see Supplemental Figure S1 at http://www.neuron.org/cgi/content/full/38/2/213/DC1).

Generation of Nogo-A/B/C Mutant Mice

We also generated a more severe allele of *nogo* by targeting the C-terminal common region in order to disrupt the transcripts of all three Nogo isoforms. We designed a gene targeting scheme to replace the first of the six common exons at the C-terminal region with a *loxP* site-flanked (floxed) neomycin resistance gene (Figure 1F). This exon was chosen for deletion because, should splicing over the selection cassette occur, a shift of open reading frame would preclude the translation of all downstream exons and might, in addition, destabilize the transcripts. The targeted allele was obtained in AB2.2 ES cells (Figure 1G). Chimeric mice were generated and bred to C57BL/6 females. Three independently targeted ES cell clones gave germline transmission. Intercrosses between heterozygous mutants gave rise to 49 wild-type, 90 heterozygous, and only 1 homozygous pup, indicating embryonic lethality of most homozygous mutants. This lethality does not appear to be caused by the neomycin resistance gene, including its *PGK* promoter, since excision of this marker gene with a Cre deleter mouse (Lewandoski et al., 1997) failed to rescue the lethality (10 +/+, 31 +/m, and 0 m/m out of 6 litters from intercrosses between heterozygotes). We did not determine the age at which lethality occurs, but assume it is before embryonic day 9.5 (E9.5), since no homozygous mutants were recovered at that stage (16 embryos scored from 2 litters).

Because the Nogo-A/B mutant was viable, these results initially suggested that the C-isoform is required for viability. However, the single viable homozygous Nogo-A/B/C mutant we obtained (the escaper, see above) proved fertile, and from it we were able to derive a line of mice in which homozygosing the mutation no longer resulted in lethality (see Experimental Procedures for details). In fact, the homozygous mutants were fertile and could be maintained as a line. Southern blot analysis of these animals showed that the gene targeting event in the original ES cell line was apparently unaffected (data not shown). Northern analysis did not detect any Nogo-A or -B isoform transcripts, presumably reflecting their destabilization (Figure 1H). A lower level of a *nogo* transcript that is slightly smaller than the wild-type *nogo-C* transcript was observed, which is as predicted for the mutated *nogo-C* transcript (also destabilized but still present) and is expected to produce no functional protein. Indeed, RT-PCR and sequence analysis confirmed that this transcript results from splicing over the neomycin cassette and, if translated, will produce a short peptide with the first 11 amino acid residues identical to those in wild-type Nogo-C but with the next 25 residues translated in a shifted frame (Figure 1I and

data not shown); importantly, the 66 amino acids in the lumenal/extracellular loop will be absent. Western analysis of whole brain extract using the anti-Nogo-A antibody demonstrated the absence of the A isoform (Figure 1J), as did immunostaining with the same antibody in the adult spinal cord (data not shown). We therefore conclude that the Nogo-A/B/C mutant likely represents a null mutant for Nogo-C and a null or severe hypomorph for Nogo-A and -B. The serendipitous derivation of this viable Nogo C-terminal mutant allowed us to assess whether regeneration is enhanced in the absence not just of the A and B isoforms but also of Nogo-C.

It is not immediately clear how an escaper line could arise from the otherwise lethal Nogo C-terminal mutation. An insight was, however, obtained when we generated two more *nogo* mutant alleles (B.Z., M.T.-L., unpublished observations). First, we obtained a doubly targeted allele in which both the N-terminal and the C-terminal region of *nogo* were targeted in *cis* (i.e., the two targeted events occurred on the same chromosome). Surprisingly, this line of mice (Nogo N/C-terminal doubly targeted allele) was homozygous viable and fertile, indicating that the targeting event at the N terminus of *nogo* rescues the lethality associated with the C-terminal mutation. Second, we generated a *nogo* deletion allele, with the genomic region between the A,B-specific exon and the first common exon deleted by Cre-mediated excision of the doubly targeted line. This allele is expected to be completely devoid of any known Nogo isoforms and almost certainly represents a clean null allele. It also proved viable and fertile (see Supplemental Table S1 at http://www.neuron.org/cgi/content/full/38/2/213/DC1). These results argue against an essential function of Nogo-C in development, which had been originally suggested by the lethality of the Nogo C-terminal mutation. Instead, these results suggest that the original C-terminal mutation might have caused misregulation of an unknown transcript at or near the *nogo* locus, which was subsequently reversed by the N-terminal mutation (and spontaneously in the viable C-terminal mutant escaper). Whatever the explanation, our deletion mutant demonstrates clearly that the *nogo* gene is not required for viability.

Inhibitory Activity of Nogo-A/B-Deficient Myelin

To assess whether Nogo-deficient myelin still inhibits neurite outgrowth, we performed in vitro neurite outgrowth assays with mouse postnatal day 7 cerebellar neurons. Myelin made from adult spinal cords of wild-type and Nogo-A/B mutant mice was used as a substrate for neurite outgrowth. As shown in Figure 2, postnatal cerebellar neurons grow extensive neurites on control wells, whereas neurite outgrow is significantly inhibited on wild-type CNS myelin. CNS myelin from Nogo-A/B mutant mice is still inhibitory, but the degree of inhibition is less than that observed with myelin from wild-type mice; about a quarter of the inhibition was lost (as measured by the length of neurites) (Figure 2E) ($p < 0.01$, Student's t test). As a positive control, an inhibitor of Rho-associated kinase (Y27632) also partially reversed the inhibitory activity of central myelin (Figure 2E, $p < 0.01$) (Dergham et al., 2002). These results indicate that Nogo-A/B contributes to the inhibitory activity of central myelin on neurite outgrowth in vitro.

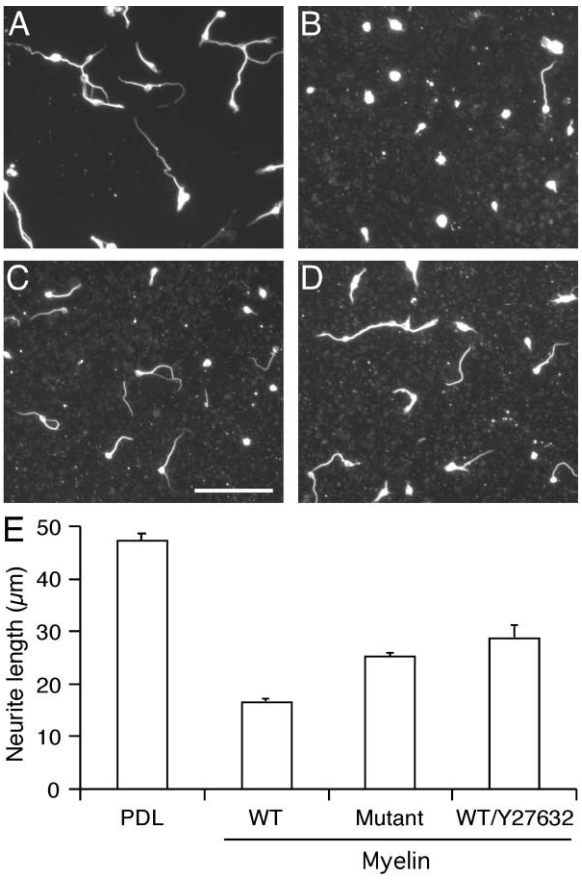

Figure 2. In Vitro Characterization of Myelin Obtained from Nogo-A/B-Deficient Mice

Mouse P7 cerebellar neurons were dissociated and plated on PDL, wild-type myelin, and Nogo-A/B mutant myelin taken from adult spinal cords. Neurons were detected with an anti-tubulin antibody (Tuj-1).

(A–D) Representative images of neurite growth under the following conditions: poly-D-lysine substrate (A), wild-type myelin substrate (B), substrate of myelin from Nogo-A/B-deficient mice (C), and wild-type myelin substrate with 10 μM Y27632 (Rho kinase inhibitor) added to the culture medium (D).

(E) Quantification of neurite outgrowth from one representative experiment out of three experiments that gave similar results. Error bars indicate SEM.

Lack of Enhanced Regeneration in Nogo-A/B Mutants

In vivo delivery of antibodies against Nogo-A in adult rats that were subjected to a spinal cord injury resulted in enhanced regeneration and sprouting of descending corticospinal tract (CST) axons (Schnell and Schwab, 1990; Bregman et al., 1995; Brosamle et al., 2000) but no enhanced regeneration of ascending sensory axons (Oudega et al., 2000). We therefore concentrated on regeneration of CST axons. In total, we examined and compared the regenerative response of 15 wild-type, 3 heterozygous, and 21 homozygous mutant animals after spinal cord injury. In all animals, a lesion of the dorsal portion of the spinal cord (dorsal hemisection) was performed at thoracic level T7-8 in adult female mice. Lesions were performed with two methods: (1) using microscissors followed by a microknife, or (2) using a 30

gauge needle to puncture the dura, followed by a microknife. These lesions resulted in the transection of the main corticospinal tracts (located in the ventral portion of the dorsal columns), as well as the lateral corticospinal tracts (sparse fibers located dorso-laterally within the white matter surrounding the spinal cord). To visualize the descending corticospinal tract axons, the tracer biotinylated dextran amine (BDA) was injected into the sensorimotor cortex at the time of the injury. In the first cohort of animals studied (five wild-type, three heterozygous, and eight homozygous mutants), BDA was injected into the cortex bilaterally. In subsequent experiments, injections were performed unilaterally to help examine whether regenerative sprouting occurred across the midline. To assess axonal regeneration, animals were sacrificed 14–19 days after injury for histological analysis, to maximize chances for detecting early stages of regeneration. Spinal cord segments either 1 or 2.5 cm long, with the lesion site approximately in the center, were sectioned in the sagittal plane (25 μm sections). All sections were collected in serial order so that individual labeled axons could be traced from section to section, allowing reconstruction of the axonal projections. In animals where only a 1 cm block was taken, additional 3 mm blocks 0.5 cm rostral and 0.5 cm caudal to the 1 cm block were sectioned in the transverse plane.

There was no systematic difference between mutant and control animals in the appearance of the lesions, although the extent varied somewhat from animal to animal. In most, lesions were as designed (i.e., they completely transected the dorsal half of the spinal cord and extended beyond the central canal, and so strictly speaking should be characterized as "dorsal over-hemisections"). Macrophages accumulated in the lesion site to a variable extent, as assessed in tissue sections (data not shown). In many animals, a dense network of presumed fibroblastic tissue was noted at the lesion site (e.g., Figures 3A and 3B).

There was no indication of a greater degree of regeneration or sprouting in the Nogo-A/B mutant animals. Indeed, we did not detect any difference in the distribution of labeled CST axons between mutants and controls. Thus, the following description applies to both, as well as to the few heterozygotes that were analyzed. (We excluded from this analysis four animals, discussed below, in which some sparing of main CST axon fibers or unusual labeling was observed).

In all animals, labeled CST axons could be seen in their normal location in the ventral part of the dorsal funiculus rostral to the lesion, although the extent of labeling varied between animals. Sample cases exhibiting substantial labeling are illustrated (Figures 3A–3D). In most cases, labeled CST axons could be followed to within 100–250 μm of the edge of the lesion, where they ended abruptly in a dense cluster of characteristic retraction bulbs (e.g., Figures 3G and 3H). When the termination of the main bundle of CST axons was visualized at high magnification, multiple branches could be seen that extended down into the underlying gray matter toward the lesion site, often taking a meandering course (Figures 3E and 3F). However, these axons for the most part ended just prior to the approximate site of injury. Their appearance was suggestive of abortive regeneration. These fine labeled axons were seen in both Nogo-

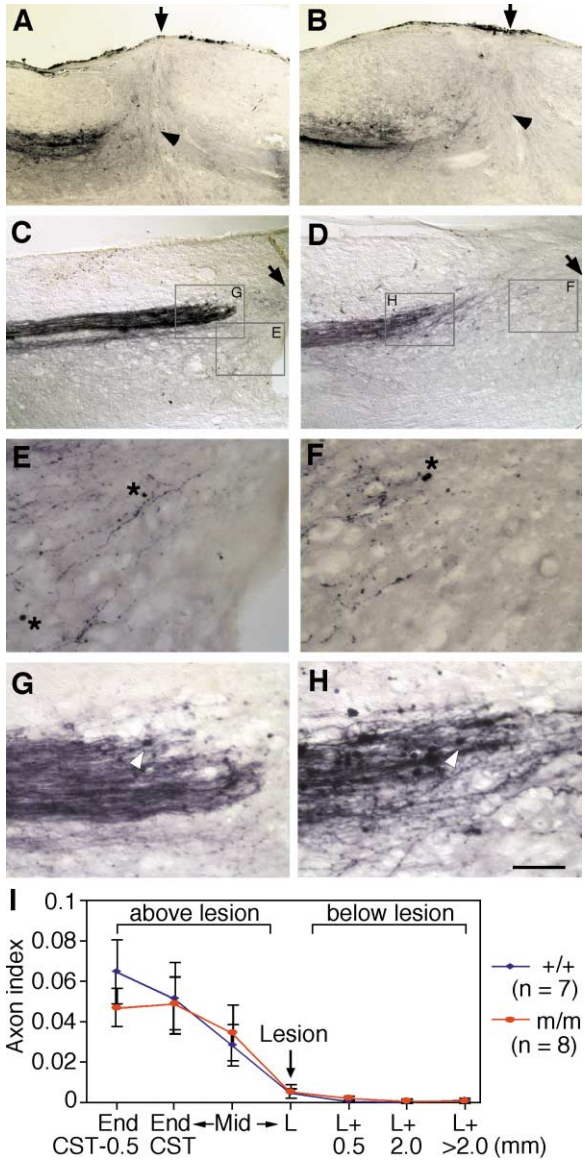

Figure 3. Absence of Enhanced Regeneration of Corticospinal Fibers in Nogo-A/B Mutant after Dorsal Hemisection Injury

(A–D) The labeled CST axons around the lesion site in representative controls (A and C) and Nogo-A/B mutants (B and D) 14–19 days after dorsal hemisection injuries. Arrows indicate the approximate location of the lesion site. In (A) and (B), arrowheads point to scar tissue at the lesion site. In (C) and (D), the lesion site is to the right and outside of the area shown. Scale bar equals 250 μm.

(E–H) High-magnification images of boxed areas in (C) and (D). (E) and (F) illustrate the axon endings and the collateral branches near the injury site. Asterisks mark stained red blood cells. (G) and (H) show the end of the main CST where characteristic retraction bulbs (some indicated by white arrowheads) can be seen. Scale bar equals 62.5 μm in (E)–(H).

(I) Quantification of the extent of regeneration in Nogo-A/B mutants and wild-type controls. *x* axis indicates specific locations along the rostrocaudal axis of the cord; *y* axis (axon index) indicates the ratio of the average number of axons counted outside the main CST at each rostrocaudal location to the numbers of fibers labeled in the medulla (mean ± SEM). L, lesion site; Mid, halfway between end of main CST and the lesion site. No statistically significant difference between numbers of sprouting or regenerating axons at any level along the rostrocaudal axis was observed between mutants and wild-type animals.

A/B mutant and control animals (Figures 3E and 3F). In a few animals of each genotype, one to three axons were observed in the distal segment below the injury site; the number and distribution was similar in mutants and controls (Figure 3I).

To assess whether subtle differences might be present, quantification of fibers in a subset of animals was undertaken. These animals were selected in a blinded manner for quantification based on the following criteria: (1) staining was of uniform high quality, (2) all sagittal sections were recovered, (3) no obviously spared main CST axons were observed, (4) the lesion site could be defined, and (5) medullary sections of high quality were obtained for normalization of tracing. Seven wild-type and eight mutant animals satisfied these criteria. The quantification method is described in Experimental Procedures. Briefly, the numbers of fibers running outside the main dorsomedial CST at different rostrocaudal levels from the lesion site were analyzed using a light microscope. In each animal, labeled axons were counted at multiple designated rostrocaudal levels in the sagittal sections running through the main CST and sections adjacent to it. To correct for interanimal tracing variability, the numbers of counted axons in each animal were normalized to the numbers of BDA-positive CST fibers in the medullary pyramid rostral to the pyramidal decussation. Quantification was performed in a blinded manner. There was no significant difference between mutants and wild-type animals in the numbers of fibers at any level (Figure 3I).

Transverse sections rostral and caudal to the lesion site were also analyzed in the 10 wild-type and 13 mutant animals that received unilateral tracer injections (Figure 4). Labeled CST axons were evident in their normal location in the ventral portion of the dorsal columns (open arrows in Figures 4A–4H) and, in most cases, between a few and dozens of labeled axons could also be seen in the dorsal portion of the lateral column (the normal location of the lateral CST, e.g., thin arrows in Figures 4F and 4H). Many collaterals extended from the main tracts ventrally into the gray matter (Figures 4B, 4D, 4F, and 4H). In many animals, a number of labeled axons crossed the midline to enter the gray matter on the side contralateral to the labeled main tract (that is, ipsilateral to the injection; see especially Figures 4J and 4L). In some animals, there were also a few labeled axons in the dorsal column on the side ipsilateral to the injection (e.g., arrowheads in Figures 4F and 4H). Although there was animal to animal variability, there was no systematic difference between Nogo-A/B mutant and control mice. While there was heavy labeling of the CST above the level of the injury (Figures 4A–4H), we did not detect any labeled fibers below the level of the injury in transverse sections in almost all Nogo-A/B mutant and control animals (e.g., Figures 4I and 4K). In one Nogo-A/B mutant and one control animal, we did observe a small number (1–3) of fibers in the transverse sections below the level of the lesion; both animals were ones in which a small number of fibers had been observed caudal to the lesion in sagittal sections (Figure 5). Thus, although hundreds of labeled axons entered the segment just rostral to the injury (too many to accurately count), almost none could be detected caudal to the injury site.

Thus, the characteristic picture seen in all animals (mutants and controls) was an abrupt end to labeled axons at the lesion site except for the fine branches that projected from the distal portion of the main CST into the adjacent gray matter. Axons in the gray matter likely represent mostly normal collateral branches to that segment, although we cannot exclude that some are regenerative sprouts. In any case, there was no systematic difference between Nogo-A/B mutant and control animals in the extent of these collaterals.

This description excluded four animals. In three of them, two wild-type and one mutant, a large cohort of labeled axons could be seen in the dorsal funiculus caudal to the lesion. These axons almost certainly were spared by the lesion, probably by being pushed aside as it was made, based on their length (several millimeters below the lesion), appearance (straight and unbranched), and location (in the normal position of the tract). In the fourth animal, a wild-type, we were surprised to observe what at first appeared to be a population of labeled axons diffusely distributed in the lateral column ipsilateral to the main labeled tract, in transverse sections rostral and caudal to the lesion site (see Supplemental Figure S2A at http://www.neuron.org/cgi/content/full/38/2/213/DC1) as well as in the sagittal sections through the lesion site (data not shown). Closer inspection revealed unusual features of these profiles: when the sections were viewed using dark field illumination, all other labeled axons reflected light but these profiles did not (Supplemental Figures S2B and S2C), and at high magnification they appeared thicker and had a "hollow" appearance (data not shown) distinct from the thin labeled fibers seen elsewhere. The nature of these stained profiles has not been established, so this animal was also excluded.

During the postsurgical survival period, we assessed the degree of behavioral impairment in a cohort of homozygous mutant and wild-type animals using the BBB assessment scale, which evaluates open field locomotor behavior (Basso et al., 1995). All the animals recovered locomoter ability to some extent over the 2 week period (see Supplemental Figure S3A at http://www.neuron.org/cgi/content/full/38/2/213/DC1), but there was no statistically significant difference between the mutants and wild-type animals in the degree of functional recovery.

The absence of regeneration in these animals contrasts with the apparently extensive regeneration observed by Dr. S. Strittmatter and colleagues in a different Nogo mutant mouse line (personal communication; see Discussion). We were concerned that the difference in these two studies could reflect a difference in the method of producing the lesion. To address this directly, Dr. S. Strittmatter generously offered to have lesions performed on our mice by a member of his laboratory, Dr. S. Li, who also performed all of the lesions in their study. Lesions were performed following the exact protocol used in analysis of their mice (for details, see their paper [Kim et al., 2003] in this issue of *Neuron*). Histological analysis was performed by Dr. S. Li and Dr. B. Zheng on the six mutant and four wild-type animals that successfully survived the procedure. This analysis failed to detect any evidence of enhanced regeneration or sprouting above or below the lesion in our mouse line (data not shown), thus indicating that the differing re-

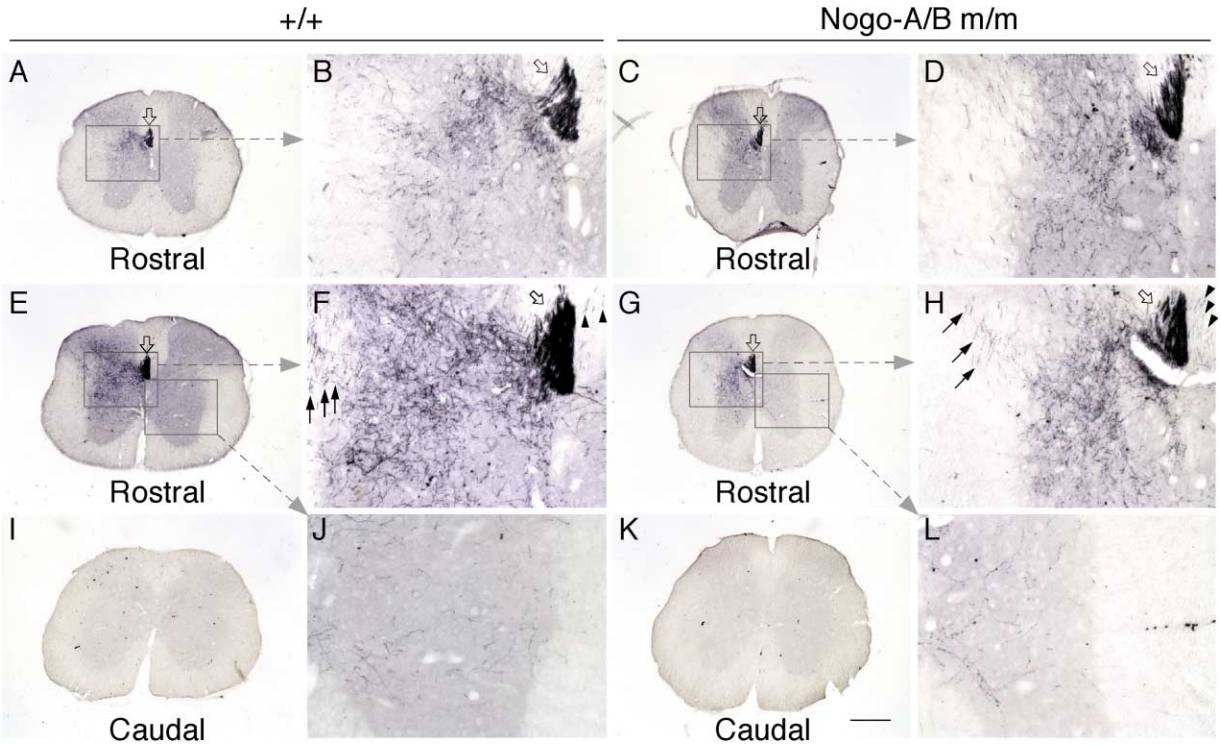

Figure 4. Distribution of Corticospinal Fibers on Transverse Sections in Segments Rostral and Caudal to the Injury in Nogo-A/B Mutant and Control Mice

(A), (C), (E), (G), (I), and (K) are transverse sections of the spinal cord taken from about 0.5 cm rostral (A, C, E, and G) or 0.5 cm caudal (I and K) to the injury site of representative wild-type (A, E, and I) and Nogo-A/B mutant (C, G, and K) mice, which received unilateral tracer injection. Animals shown in (A) and (C) correspond to those shown in Figures 3C and 3D, respectively. (E) and (I) are from the same wild-type animal; (G) and (K) are from the same mutant animal. Scale bar equals 300 μm.

(B), (D), (F), (H), (J), and (L) are high-magnification images of the boxed areas in (A), (C), (E), and (G). Open arrows in (A)–(H) indicate the labeled main CST (in the ventral part of the dorsal column on the left hand side). (B), (D), (F), and (H) show the heavily labeled main CST (open arrows) and many labeled collaterals distributed throughout the gray matter. In (F) and (H), thin arrows indicate the small population of labeled axons in the dorsal part of the lateral column at the normal location of the lateral CST; black arrowheads indicate the few main CST axons labeled ispilateral to the injection site. (J) and (L) show some labeled axons in the gray matter contralateral to the labeled main CST. Note that there are hundreds of labeled axons evident in the rostral segments (E and G), whereas no labeled axons are detectable in the caudal segments (I and K). Scale bar equals 60 μm.

sults between the two laboratories likely reflect differences between mouse lines rather than differences in surgical protocols.

Lack of Enhanced Regeneration in Nogo-A/B/C Mutants

The C isoform of Nogo is also expressed in the central nervous system (Huber et al., 2002), raising the question whether removal of that isoform, along with the A/B isoforms, could cause greater regeneration than that seen in our Nogo-A/B mutant animals. We performed spinal cord lesions in Nogo-A/B/C mutant mice obtained from breeding the one initial escaper, and we examined the corticospinal projection for regeneration. For this experiment, animals were allowed to survive for longer periods following the spinal cord injury (9 weeks) in case the failure to detect regeneration was due to the short postinjury survival period. Thus, animals received bilateral BDA injections 7 weeks after the spinal cord injury (and 2 weeks prior to being sacrificed). Eight wild-type and eight mutant animals that survived the procedure were analyzed.

Assessment of locomotor function using the BBB rating scale revealed that Nogo-A/B/C mutant animals on average exhibited slightly better locomotor function (especially at the first two time points), but the difference between groups was not statistically significant at any time point (see Supplemental Figure S3B at http://www.neuron.org/cgi/content/full/38/2/213/DC1). Assessment of the distribution of the CST in Nogo-A/B/C mutants again revealed no differences between mutants and controls. The CST ended abruptly just rostral to the lesion site in characteristic retraction bulbs (Figures 5A and 5B). A few axon collaterals could be seen just rostral to the terminal end bulbs, and these extended down into the underlying gray matter (Figures 5A and 5B).

Evaluation of transverse sections from mutant and control animals revealed heavy labeling of the CST above the level of the injury; again, hundreds of labeled axons entered the segment rostral to the injury (for examples, see Figures 5C and 5D). At the same time, in all animals but one there were no labeled axons below the level of the injury (Figures 5E and 5F). In the one exceptional case (Figure 5F), which was a mutant, we

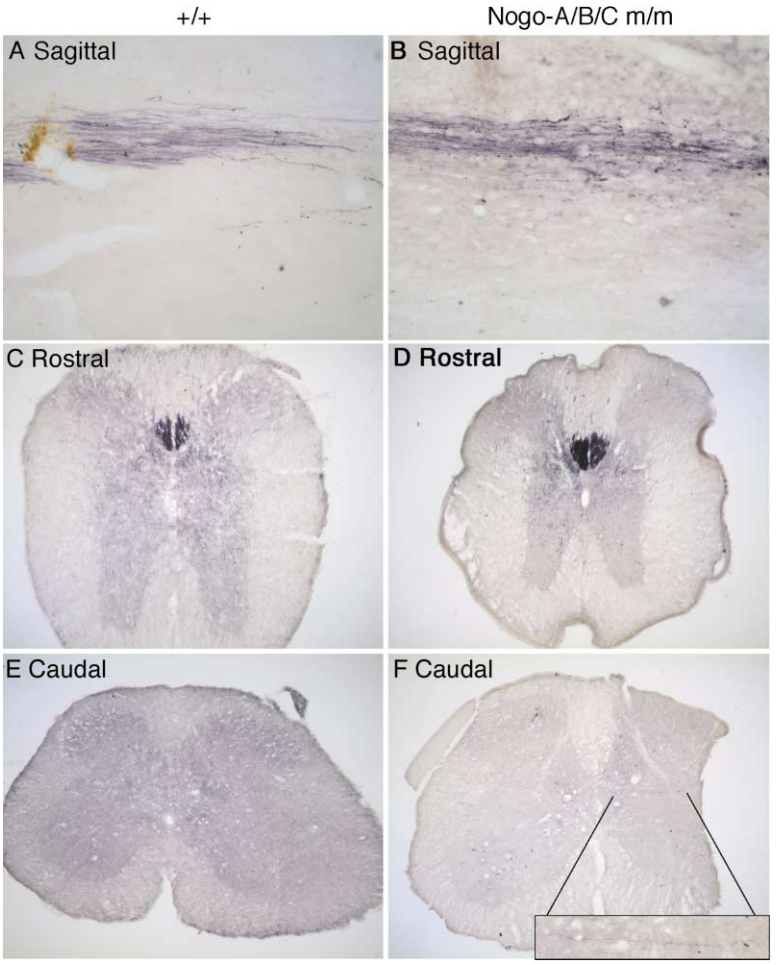

Figure 5. Distribution of Corticospinal Fibers in Injured Nogo-A/B/C Mutant and Control Mice

The photomicrographs illustrate the distribution of labeled CST axons in representative control and Nogo-A/B/C mutant animals, which received bilateral tracer injection. Genotypes are indicated on the top. (A) and (B) illustrate representative sagittal sections just rostral to the injury site; (C) and (D) illustrate transverse sections taken approximately 0.5 cm rostral to the injury. (E) and (F) illustrate sections taken approximately 0.5 cm caudal to the injury. Note that there are hundreds of labeled axons evident in the rostral segments, whereas only one labeled axon was detected in the caudal sections taken from any of the cases. This single example of a labeled axon caudal to the injury is illustrated in the high-magnification inset in (F).

did detect a single labeled axon in the caudal segment (see high-magnification inset in Figure 5F). We were not able to trace this axon through more rostral segments, and so we were unable to define its course to determine whether it was spared or had regenerated.

Discussion

Nogo has been implicated in regenerative failure in the central nervous system through antibody perturbation studies (Schnell and Schwab, 1990; Bregman et al., 1995; Thallmair et al., 1998; Brosamle et al., 2000). We have generated mutant mice that lack Nogo-A/B or -A/B/C expression, but we did not detect an enhancement of regeneration of corticospinal tract axons following the same type of dorsal column lesion that was used in the antibody delivery experiments. In fact, any evidence of minimal regeneration, including apparent collateral sprouting rostral to the lesion, and occasional axons below the lesion site in some animals, was seen in both mutant and wild-type animals. Quantification also failed to detect any statistically significant difference in the number of labeled fibers between wild-type and mutant animals at various rostral-caudal levels relative to the lesion site. Although we found that the absence of Nogo-A/B in these animals reduced the amount of inhibitory activity of myelin substrates tested in vitro—confirming that Nogo-A/B contributes to inhibition in vitro—our results imply that loss of Nogo-A/B is not sufficient to permit significant regeneration in vivo, presumably either because Nogo's in vitro activity does not reflect a physiological role for Nogo in blocking regeneration in vivo, or because other inhibitors are sufficient to block regeneration.

What accounts for the difference between our studies and the antibody perturbation experiments? In those studies, the IN-1 monoclonal antibody was initially delivered through implantation of the IN-1 hybridoma cell line into the cortex in rats and led to regeneration of a small number of fibers past the lesion site following a bilateral CST lesion (Schnell and Schwab, 1990), as well as to increased compensatory sprouting of unlesioned axons following a unilateral CST lesion (Thallmair et al., 1998). Subsequently, large amounts of IN-1 Fab fragments were directly infused into the injury site and stimulated regeneration past the lesion in about 60% of rats in short term ($\sim$2 week) dorsal hemisection studies (Brosamle et al., 2000). Although striking, these studies are limited by the fact that IN-1 is not specific for Nogo and reacts with multiple molecular species (Spillmann et al., 1998), making its target uncertain. More specific antibodies have been made (Chen et al., 2000), but their in vivo effects have not yet been reported. In addition, it is not understood at present why evidence of regeneration

was found in only a subset of animals, and why IN-1 failed to stimulate regeneration of lesioned sensory axons in the dorsal columns (Oudega et al., 2000), despite the fact that IN-1 dramatically improves sensory axon growth on myelin in vitro (e.g., Chen et al., 2000).

In our studies, similar techniques were used to produce CST lesions and to trace CST axons, yet animals lacking Nogo-A/B did not exhibit any evidence of enhanced regeneration 14–19 days after a lesion. We also did not observe any evidence of enhanced sprouting of CST axons above the lesion site (e.g., enhanced contralateral projections) in the mutants compared to the controls. The absence of either regeneration or sprouting is in line with the lack of improvement in the BBB behavioral score in mutant animals compared to controls.

There are two possible explanations for the discrepancy between our results and those obtained in the antibody perturbation experiments.

First, it is possible that in the antibody perturbation experiments, regeneration was stimulated not by inhibition of Nogo, but by IN-1 interfering with one of the distinct molecular species detected by the IN-1 antibody (Spillmann et al., 1998). In this scenario, Nogo-A/B does not contribute significantly to regeneration block in the normal adult nervous system.

Second, IN-1 may have produced its effects by interfering with Nogo function. If so, our failure to detect regeneration in our Nogo knockout mice could be explained by one or more of the following possibilities. (1) It is possible that only a subpopulation of CST axons regenerated, and that we failed to label that population. This seems unlikely, given the extent of labeling in our studies. (2) The specific surgical paradigm we used may have made regeneration more difficult. This again seems unlikely, since the techniques used were similar (if not identical) and since no regeneration was observed in our Nogo-A/B mutants when they were lesioned by Dr. S. Li using a protocol that apparently allowed regeneration in a line of mice analyzed by him in Dr. Strittmatter's laboratory. (3) Our studies were performed in mice, whereas the antibody treatment studies were performed in rats. It is conceivable that more regeneration could be observed in a different species or in a different genetic background (ours was mixed, about three-quarters C57BL/6 and one-quarter 129S7). (4) The antibody treatment was acute, whereas our genetic deletion was present through development. It is conceivable that compensatory changes occurred in the mutant mice that diminished regenerative capacity. (5) We also considered the possibility that the absence of a regenerative response in Nogo-A/B mutants might be due to the presence of the Nogo-C isoform (although the antibody targeted Nogo-A specifically). We therefore generated mice in which all three isoforms are mutated through targeting of the C-terminal common region. Although we initially found that these mutants are embryonic lethal, we did obtain one viable homozygous mouse from which we were able to derive a line of mice that apparently lack Nogo-A, -B, and -C. However, no evidence of enhanced regeneration or sprouting in these animals was observed either.

Thus, if a regenerative response of CST axons is possible in the absence of Nogo-A, -B, and -C in mice, our results imply that this may (1) involve a subpopulation of axons not labeled in our studies, (2) require some specific type of lesion different from the one we or Dr. Strittmatter's laboratory performed, or (3) require a particular genetic background different from the one we used. If highly restrictive conditions like these are required for a successful regenerative response, then the relevance to regeneration following traumatic injury to the spinal cord might be limited.

A similar discrepancy is also apparent in the different results obtained in studies of mice with different mutations of the *nogo* gene reported by two other groups in companion papers in this issue of *Neuron* (Kim et al., 2003; Simonen et al., 2003). In both studies, the large Nogo-A-specific exon was disrupted (although different effects were observed on expression of the Nogo-B isoform).

First, Dr. S. Strittmatter and colleagues (Kim et al., 2003) have analyzed a mutant mouse in which the large Nogo-A-specific exon is disrupted as a result of a gene trap insertion; while the trapping vector was inserted into a Nogo-A-specific exon, the consequences of this insertion for Nogo expression (assessed by Northern and Western analyses) are apparently similar to our Nogo-A/B mutant. Specifically, both Nogo-A and -B expression appear to be disrupted (Nogo-C expression is apparently unchanged). After a lesion, they observed extensive sprouting and regeneration that are most pronounced on the side contralateral to the labeled corticospinal tract, although it is uncertain whether this is true in adult animals or only in young ones (personal communication).

It is difficult to account for the remarkable divergence between our study and theirs. We studied both young and old animals (the median age was young [8 weeks]), but we saw no regeneration or enhanced sprouting. We do not believe that differences in surgical or labeling techniques can explain the difference, since similar techniques were used by both groups and since Dr. Strittmatter reports extensive sprouting far rostral to the lesion, which should be insensitive to the precise lesion techniques that are used.

We are thus left with three possible explanations for the discrepancy. The first is differences in genetic backgrounds; however, if this is the explanation, it again calls into question the robustness of regeneration that is possible following loss of Nogo function. The second is that in our mutant, but not Dr. Strittmatter's, some compensatory change occurred that suppressed regeneration. The third is that Dr. Strittmatter's phenotype reflects more than a loss of Nogo function. The mutation they analyzed was generated by Lexicon Genetics by random insertion of a complex gene trap vector containing a strong promoter (Zambrowicz et al., 1998), and it is possible that this has resulted in alteration or deregulation of other neighboring genetic loci, with regeneration being caused secondarily by this change.

Second, Dr. M. Schwab and colleagues (Simonen et al., 2003) generated a distinct mutant in which the same large Nogo-A-specific exon was disrupted by conventional gene targeting. This results in loss of Nogo-A but also a dramatic upregulation in Nogo-B expression in spite of the fact that this mutation disrupts the same exon as that trapped in the mutant analyzed by Dr. Strittmatter and colleagues. In this mutant, very limited

though consistent regeneration was observed, but without the lateralized effect observed by Dr. Strittmatter (personal communication). While this result is consistent with Nogo-A contributing to regeneration failure, it would seem to imply a modest role for Nogo-A alone. As well, it is conceivable that the phenotype reflects a gain-of-function phenotype from deregulation of Nogo-B expression.

Thus, future studies are required to determine whether the differences between our results and those of the other two groups reflect some limitation of our models, or instead reflect the fact that something more than loss of Nogo-A and/or -B is occurring in their models. The possibility of complex genetic interactions following disruption of the *nogo* locus is highlighted by the opposite effects on Nogo-B expression of the two mutations analyzed by the other two groups (even though the same exon was disrupted in both), and by the complexity in the pattern of lethality in our four Nogo mutants (with a C-terminal mutation initially causing lethality that was reversed both spontaneously and by a second N-terminal mutation; see Supplemental Table S1 at http://www.neuron.org/cgi/content/full/38/2/213/DC1).

Whatever the explanation for the different degrees of regeneration observed in the three studies, our results nonetheless demonstrate that removal of Nogo-A and -B, or of all three isoforms, is not sufficient to allow extensive regeneration or sprouting of corticospinal tract axons following injury, and thus raise questions as to the normal contribution of Nogo to regeneration failure. Future studies will determine whether a greater regenerative response in our animals can be observed under other circumstances, in particular whether removal of other inhibitors like MAG or OMgp in addition to Nogo results in an enhanced regenerative response.

Experimental Procedures

Gene Targeting at the *nogo* Locus

Two overlapping clones covering the N-terminal exon and four overlapping clones covering the C-terminal common exons of *nogo* were isolated from a mouse 129S5 (coisogenic to 129S7) genomic library. To target the N terminus to generate Nogo-A/B mutants, a replacement vector was constructed with an Frt-flanked *PGK-Hprt* minigene as the positive selection marker and *HSVTK* as the negative selection marker. A fusion reporter gene *IRES-GFPLacZ* and a *loxP* site were also included in the targeting vector. A 1 kb genomic fragment between the *Nco*I site in exon 1 and the first *Bam*HI site in intron 1 was deleted. The targeting vector was electroporated into AB2.2 ES cells. A 0.6 kb 5′ external probe was used to detect targeted ES cell clones. From 90 ES cell clones screened by Southern blot, 53 targeted clones were identified.

To target the Nogo C-terminal region to generate Nogo-A/B/C mutants, a replacement vector was constructed with a floxed neomycin resistance gene as the positive selection marker and *HSVTK* as the negative selection marker. The two *loxP* sites in this vector are in the same orientation as the one in the N-terminal targeting vector described above when targeted at the *nogo* locus, so that a deletion can be made from a doubly targeted allele with Cre-mediated excision. A 1.9 kb *Sac*I-*Hind*III genomic fragment containing the first common exon was deleted. A 1.5 kb 5′ external probe was used to detect targeted ES cell clones. Among 180 ES cell clones screened by Southern blot, 12 targeted clones were identified. Heterozygous Nogo-A/B/C mutant mice were derived from three of these ES cell lines. As described in the text, intercrosses of these mice generally failed to yield any viable homozygous progeny, except for a single escaper—a homozygous male pup that grew to adulthood. While most of our intercrosses were between (C57BL/6 × 129S7) F1 heterozygotes, this escaper arose from a (F1 × chimera) mating. Mating of this homozygous escaper to heterozygous females gave rise to heterozygous and homozygous progeny in a ratio that deviates from 1:1 (45 +/m and 14 m/m), indicating the continued presence of some inviable homozygous progeny. Five heterozygous progeny that derived from the escaper were expanded clonally (each presumably carrying one of the two mutant alleles from the escaper), three of which, when intercrossed, readily gave rise to viable and fertile homozygotes, while the other two continued to produce inviable homozygous progeny.

We subsequently targeted the *nogo* N terminus through a second gene targeting event in an ES cell line that already carried the targeted C-terminal mutation that had proved to be homozygous lethal in mice (this particular ES cell line was different from the one from which the escaper derived). This resulted in an ES cell line that carries both Nogo N- and C-terminal mutations on the same chromosome (the doubly targeted allele). Upon transmission through the germline, homozygous doubly targeted Nogo mutants were readily obtained from intercrosses between heterozygotes. A full *nogo* deletion allele was generated by breeding the doubly targeted allele to a Cre deleter line (Lewandoski et al., 1997) and was also viable.

Western Blot and Immunocytochemistry

A peptide specific to the A isoform of mouse Nogo, SYDGIKLEPENP PPYEEA, was used to generate rabbit anti-Nogo-A polyclonal antibodies. This peptide corresponded to that used previously to generate an antibody to rat Nogo-A (Chen et al., 2000), with one amino acid difference. Antiserum was affinity purified with the same peptide and used for Western blot analysis (1:500 dilution), using an HRP-conjugated goat anti-rabbit secondary antibody. Both antiserum and purified antibody were used for immunohistochemistry at a 1:300 dilution, using a FITC-conjugated goat anti-rabbit secondary antibody. Nogo-B was detected with a commercial antibody directed against the N terminus of Nogo-A/B (Santa Cruz).

Neurite Outgrowth Assay

Myelin was prepared from mouse spinal cords as described (Colman et al., 1982). Eight-well chamber slides were precoated with poly-D-lysine, coated with myelin (1 mg total protein per well), and dried overnight, then exposed to laminin (3 μg/ml) for 2 hr. Mouse P7 cerebellar cells were prepared as described (Wang et al., 2002), plated at a density of 5×10^4 cells/well, incubated for 22 hr, then fixed and stained with an anti-tubulin antibody (TuJ1, Covance). Neurite lengths were measured from a total of about 400–500 neurons on six representative images taken per well; 3 wells per condition.

Surgery and Care of Animals

All Nogo-A/B mutants and their controls that were analyzed were in a (C57BL/6 × 129S7) N2 background. All Nogo-A/B, Nogo-A/B/C mutants, and their controls that were analyzed were in a (C57BL/6 × 129S7) NE2 background. Female mice 6 to 14 weeks old (most were 6 to 10 weeks old), age-matched between genotypes, were anesthetized with Avertin (1.3% tribromoethanol and 0.8% amyl alcohol; Sigma-Aldrich, St. Louis, MO). The hair on the back was shaved and swabbed with Betadine. A midline incision was made over the thoracic vertebrae, the paravertebral muscles were separated from the vertebral column and retracted, and a laminectomy was performed at the desired level (T7-8). Dorsal hemisection injuries were produced in one of two ways. For the experiments involving Nogo-A/B/C mutants and their littermate controls, a fine microknife was lowered 0.7 mm into the cord near the midline to the level of the central canal. The microknife was then drawn across the dorsal aspect of the spinal cord through the dura. The procedure was then repeated going in the opposite direction. For the experiments involving the Nogo-A/B mutant animals and their controls, the dorsal spinal cord was first either cut with a pair of microscissors, or the dura was punctured with a 30 gauge needle bilaterally on the lateral aspects of the cord; in either case, this was followed by drawing a fine microknife through the dorsal spinal cord to assure complete hemisection. After hemostasis was achieved, the muscle layers and the skin were sutured.

For short-term experiments, after closure of the wound, animals were passed to a second surgical station where they received injections of tetramethylrhodamine and biotin-conjugated dextran, 10,000 MW, lysine fixable (mini-ruby, Molecular Probes) into the sensorimotor cortex. In one set of experiments, animals received bilateral injections; in the second the animals received unilateral injections. In most experiments, two injections were made per hemisphere, delivering 0.5 μl of a 10% solution of BDA at the following coordinates: Site 1, 1.0 mm lateral, 0.5 anterior to bregma, 0.5 mm deep to the cortical surface; Site 2, 1.0 mm lateral, 0.5 posterior to bregma, 0.5 mm deep to the cortical surface. In other experiments including the one that was done in Dr. Strittmatter's laboratory, three injections were made surrounding the site 1.0 mm lateral and 1.0 mm posterior to bregma. After completion of the injections, the scalp was sutured. The entire operative procedure, including spinal cord lesion and injection, took approximately 45 min. For long-term experiments, the tracer injection was done on a separate day 7 weeks after the dorsal hemisection.

The animals were placed on soft bedding on a heating pad until they had recovered fully from the anesthetic. The animals received injections of the antibiotic Baytril once daily for two weeks postoperatively to prevent urinary tract infection. Urine was expelled by manual abdominal pressure twice daily for seven days, then once daily until bladder function was restored or the conclusion of the experiment. All procedures were approved by the Institutional Animal Care and Use Committee at UC Irvine and the Administrative Panel on Laboratory Animal Care at Stanford.

Histology

At the specified postinjury times, the mice received an overdose of the anesthetic nembutal and were perfused transcardially with 4% paraformaldehyde in 1× PBS (phosphate-buffered saline). The brains and spinal cords were removed and post-fixed by immersion overnight in the same fixative. On the following day, the spinal cords were placed in 30% sucrose overnight for cryoprotection and were then prepared in one of two ways. For one group of animals, a 2.5 cm block surrounding the injury site was embedded in OCT and frozen. These cords were sectioned in the sagittal plane, collecting every section in buffer or on slides. In a second group, a 1 cm block was taken that extended 5 mm rostral and 5 mm caudal to the center of the injury. This block was sectioned in the sagittal plane, collecting every section. The rostral and caudal segments were embedded and frozen separately, and were sectioned in the transverse plane. The tracer was visualized by staining with the HRP-based Vectastain ABC system (Vector Laboratories) with DAB as the chromogen.

Quantification

The number of labeled axons in the dorsomedial CST at different rostrocaudal levels from the lesion site was analyzed by light microscopy. On sagittal sections at 400× magnification, the number of intersections of BDA-labeled fibers with a dorsoventral line was counted. Five to six sagittal sections, including the section through the most midline portion of the main dorsal medial CST and the 2–3 adjacent section on either side of the midline section, were selected for each animal. Only those fibers running outside the main thick bundle of CST axons were counted. To normalize for individual tracing variability, the number of BDA-positive CST fibers was determined by counting fibers at 1000× magnification in a transverse section of the medulla in the pyramidal tract rostral to the pyramidal decussation. The number of fibers at different distances from the lesion site was averaged over the 5–6 sagittal sections and divided by the number of labeled CST fibers in the medulla for each animal. Statistical comparison was done with the two-tailed t test.

Acknowledgments

We thank J. Mak for blastocyst injections, N. Velarde for colony maintenance and genotyping, R. Gonzalez for expert assistance in dorsal hemisection, and K. Matsudaira Yee for tissue processing; H. Lin, K. Banos, G. Bernal, A. Gorjian, D. Inman, K. Sharp, C. Chechelski, and J. Zhong for technical assistance; A. Anderson and J. Weimann for technical advice; X. Wang for the *IRES-GFPLacZ* cassette and A. Bradley for AB2.2 ES cells; G. Martin for the Cre deleter mouse line; Z. He and K. Wang for sharing reagents and protocols; S. McConnell for sharing surgical equipment; and F. Bradke, J. Atwal, and other members of the M.T.-L. laboratory for helpful discussions. We thank Drs. S. Strittmatter and M. Schwab for extensive discussions on experimental procedures and for sharing their unpublished data prior to publication. We thank Dr. Strittmatter further for allowing the analysis of our mice in his laboratory by his postdoctoral fellow, Dr. S. Li, and J.-E. Kim for help with those experiments as well. We also thank Dr. Schwab and Dr. V. Pedersen for sharing their method for quantifying regeneration, and for helping us to apply it in our study (Figure 3l). B.Z. is supported by a Helen Hay Whitney Fellowship. Supported by a grant from the International Spinal Research Trust and by the Roman Reed Spinal Cord Injury Research Fund of California. M.T.-L. is an Investigator of the Howard Hughes Medical Institute.

Received: October 21, 2002
Revised: March 11, 2003
Accepted: March 18, 2003
Published: April 23, 2003

References

Bartsch, U., Bandtlow, C.E., Schnell, L., Bartsch, S., Spillmann, A.A., Rubin, B.P., Hillenbrand, R., Montag, D., Schwab, M.E., and Schachner, M. (1995). Lack of evidence that myelin-associated glycoprotein is a major inhibitor of axonal regeneration in the CNS. Neuron *15*, 1375–1381.

Basso, D.M., Beattie, M.S., and Bresnahan, J.C. (1995). A sensitive and reliable locomotor rating scale for open field testing in rats. J. Neurotrauma *12*, 1–21.

Bradbury, E.J., Moon, L.D., Popat, R.J., King, V.R., Bennett, G.S., Patel, P.N., Fawcett, J.W., and McMahon, S.B. (2002). Chondroitinase ABC promotes functional recovery after spinal cord injury. Nature *416*, 636–640.

Bregman, B.S., Kunkel-Bagden, E., Schnell, L., Dai, H.N., Gao, D., and Schwab, M.E. (1995). Recovery from spinal cord injury mediated by antibodies to neurite growth inhibitors. Nature *378*, 498–501.

Brosamle, C., Huber, A.B., Fiedler, M., Skerra, A., and Schwab, M.E. (2000). Regeneration of lesioned corticospinal tract fibers in the adult rat induced by a recombinant, humanized IN-1 antibody fragment. J. Neurosci. *20*, 8061–8068.

Caroni, P., and Schwab, M.E. (1988). Antibody against myelin-associated inhibitor of neurite growth neutralizes nonpermissive substrate properties of CNS white matter. Neuron *1*, 85–96.

Chen, M.S., Huber, A.B., van der Haar, M.E., Frank, M., Schnell, L., Spillmann, A.A., Christ, F., and Schwab, M.E. (2000). Nogo-A is a myelin-associated neurite outgrowth inhibitor and an antigen for monoclonal antibody IN-1. Nature *403*, 434–439.

Colman, D.R., Kreibich, G., Frey, A.B., and Sabatini, D.D. (1982). Synthesis and incorporation of myelin polypeptides into CNS myelin. J. Cell Biol. *95*, 598–608.

Dergham, P., Ellezam, B., Essagian, C., Avedissian, H., Lubell, W.D., and McKerracher, L. (2002). Rho signaling pathway targeted to promote spinal cord repair. J. Neurosci. *22*, 6570–6577.

Domeniconi, M., Cao, Z., Spencer, T., Sivasankaran, R., Wang, K., Nikulina, E., Kimura, N., Cai, H., Deng, K., Gao, Y., et al. (2002). Myelin-associated glycoprotein interacts with the Nogo66 receptor to inhibit neurite outgrowth. Neuron *35*, 283–290.

Fawcett, J.W. (1992). Intrinsic neuronal determinants of regeneration. Trends Neurosci. *15*, 5–8.

Fitch, M.T., and Silver, J. (1997). Glial cell extracellular matrix: boundaries for axon growth in development and regeneration. Cell Tissue Res. *290*, 379–384.

Fournier, A.E., GrandPré, T., and Strittmatter, S.M. (2001). Identification of a receptor mediating Nogo-66 inhibition of axonal regeneration. Nature *409*, 341–346.

Goldberg, J.L., Klassen, M.P., Hua, Y., and Barres, B.A. (2002). Amacrine-signaled loss of intrinsic axon growth ability by retinal ganglion cells. Science *296*, 1860–1864.

GrandPré, T., Nakamura, F., Vartanian, T., and Strittmatter, S.M. (2000). Identification of the Nogo inhibitor of axon regeneration as a Reticulon protein. Nature *403*, 439–444.

GrandPré, T., Li, S., and Strittmatter, S.M. (2002). Nogo-66 receptor antagonist peptide promotes axonal regeneration. Nature *417*, 547–551.

Huber, A.B., Weinmann, O., Brosamle, C., Oertle, T., and Schwab, M.E. (2002). Patterns of Nogo mRNA and protein expression in the developing and adult rat and after CNS lesions. J. Neurosci. *22*, 3553–3567.

Jakeman, L.B., and Reier, P.J. (1991). Axonal projections between fetal spinal cord transplants and the adult rat spinal cord: a neuroanatomical tracing study of local interactions. J. Comp. Neurol. *307*, 311–334.

Kim, J.-E., Li, S., GrandPré, T., Qiu, D., and Strittmatter, S.M. (2003). Axon regeneration in young adult mice lacking Nogo-A/B. Neuron *38*, this issue, 187–199.

Lewandoski, M., Meyers, E.N., and Martin, G.R. (1997). Analysis of *Fgf8* gene function in vertebrate development. Cold Spring Harb. Symp. Quant. Biol. *62*, 159–168.

Li, M., Shibata, A., Li, C., Braun, P.E., McKerracher, L., Roder, J., Kater, S.B., and David, S. (1996). Myelin-associated glycoprotein inhibits neurite/axon growth and causes growth cone collapse. J. Neurosci. Res. *46*, 404–414.

Liu, B.P., Fournier, A., GrandPré, T., and Strittmatter, S.M. (2002). Myelin-associated glycoprotein as a functional ligand for the Nogo-66 receptor. Science *297*, 1190–1193.

McKerracher, L., David, S., Jackson, D.L., Kottis, V., Dunn, R.J., and Braun, P.E. (1994). Identification of myelin-associated glycoprotein as a major myelin-derived inhibitor of neurite growth. Neuron *13*, 805–811.

Mukhopadhyay, G., Doherty, P., Walsh, F.S., Crocker, P.R., and Filbin, M.T. (1994). A novel role for myelin-associated glycoprotein as an inhibitor of axonal regeneration. Neuron *13*, 757–767.

Oudega, M., Rosano, C., Sadi, D., Wood, P.M., Schwab, M.E., and Hagg, T. (2000). Neutralizing antibodies against neurite growth inhibitor NI-35/250 do not promote regeneration of sensory axons in the adult rat spinal cord. Neuroscience *100*, 873–883.

Pasterkamp, R.J., Giger, R.J., Ruitenberg, M.J., Holtmaat, A., De Wit, J., De Winter, F., and Verhaagen, J. (1999). Expression of the gene encoding the chemorepellent semaphorin III is induced in the fibroblast component of neural scar tissue formed following injuries of adult but not neonatal CNS. Mol. Cell. Neurosci. *13*, 143–166.

Prinjha, R., Moore, S.E., Vinson, M., Blake, S., Morrow, R., Christie, G., Michalovich, D., Simmons, D.L., and Walsh, F.S. (2000). Inhibitor of neurite outgrowth in humans. Nature *403*, 383–384.

Ramon y Cajal, S. (1928). Degeneration and Regeneration of the Nervous System, translated by R.M. May (New York: Oxford University Press).

Schnell, L., and Schwab, M.E. (1990). Axonal regeneration in the rat spinal cord produced by an antibody against myelin-associated neurite growth inhibitors. Nature *343*, 269–272.

Schwab, M.E., and Bartholdi, D. (1996). Degeneration and regeneration of axons in the lesioned spinal cord. Physiol. Rev. *76*, 319–370.

Schwab, M.E., and Caroni, P. (1988). Oligodendrocytes and CNS myelin are nonpermissive substrates for neurite growth and fibroblast spreading in vitro. J. Neurosci. *8*, 2381–2393.

Simonen, M., Pedersen, V., Weinmann, O., Schnell, L., Buss, A., Ledermann, B., Christ, F., Sansig, G., van der Putten, H., and Schwab, M.E. (2003). Systemic deletion of the myelin-associated outgrowth inhibitor Nogo-A improves regenerative and plastic responses after spinal cord injury. Neuron *38*, this issue, 201–211.

Spillmann, A.A., Bandtlow, C.E., Lottspeich, F., Keller, F., and Schwab, M.E. (1998). Identification and characterization of a bovine neurite growth inhibitor (bNI-220). J. Biol. Chem. *273*, 19283–19293.

Thallmair, M., Metz, G.A., Z'Graggen, W.J., Raineteau, O., Kartje, G.L., and Schwab, M.E. (1998). Neurite growth inhibitors restrict plasticity and functional recovery following corticospinal tract lesions. Nat. Neurosci. *1*, 124–131.

Wang, K.C., Koprivica, V., Kim, J.A., Sivasankaran, R., Guo, Y., Neve, R.L., and He, Z. (2002). Oligodendrocyte-myelin glycoprotein is a Nogo receptor ligand that inhibits neurite outgrowth. Nature *417*, 941–944.

Zambrowicz, B.P., Friedrich, G.A., Buxton, E.C., Lilleberg, S.L., Person, C., and Sands, A.T. (1998). Disruption and sequence identification of 2,000 genes in mouse embryonic stem cells. Nature *392*, 608–611.